

Quantitative sense-specific determination of murine coronavirus RNA by reverse transcription polymerase chain reaction

Barry Schoenike ^{a,b}, Amy K. Franta ^{a,b}, John O. Fleming ^{a,b,*}

^a *Departments of Neurology and Medical Microbiology and Immunology, University of Wisconsin, 1300 University Avenue, Madison, WI 53906, USA*

^b *William s. Middleton Veterans Hospital, Madison, WI 53792, USA*

Received 1 July 1998; received in revised form 10 November 1998; accepted 13 November 1998

Abstract

In many applications, it is useful to know the sense and amount of viral RNAs present in a sample. In theory, sense-specific measurement of viral RNAs may be achieved by reverse transcription polymerase chain reaction (RT-PCR) assays which utilize primers of defined polarity during the RT step. However, in practice, it has been shown that such assays are prone to artifacts, such as non-specific priming, which drastically diminish their reliability. Using murine coronavirus MHV-4 as a model, we describe and validate several modifications of the RT-PCR procedure which eliminate these artifacts. Key RT-PCR parameters which were optimized include the design of tagged primers, DNase treatment of in vitro transcribed RNA standards, specification of temperature differences between RT and PCR annealing steps, and use of competitive RNA templates for quantitative assays. The assays described may be used to determine the sense and abundance of any viral or host RNA of interest in complex biological specimens. © 1999 Elsevier Science B.V. All rights reserved.

Keywords: PCR; Sense-specific RNA determination; Mouse hepatitis virus; Coronaviruses

1. Introduction

In the course of many experiments in virology, it is of interest to determine the sense and amount

of viral RNAs. For example, in the case of viruses with a RNA genome, the presence of RNAs of antigenomic sense usually indicates active viral transcription. In other studies, in which viral gene expression appears altered, it would be informative to determine whether this change is correlated with corresponding alterations in the level of pos-

* Corresponding author. Tel.: +1-608-263-5421; fax: +1-608-263-0412; e-mail: fleming@neurology.wisc.edu.

itive or negative sense viral RNA. A striking change in the expected relative or absolute abundance of viral RNA of a given sense may provide clues as to the mode of viral replication *in vitro* or of viral pathogenesis *in vivo*.

In some applications, the sense of viral RNAs present in a sample may be determined unambiguously by Northern blotting utilizing sense-specific probes. However, in many experiments, particularly with samples obtained *in vivo*, viral RNA may not be of sufficiently high concentration to allow detection by this technique. Clearly, RT-PCR assays provide high sensitivity (approximately 3–4 logs more than Northern blot or nuclease protection assays) (Foley et al., 1993; Ausubel et al., 1994; Köhler et al., 1995) and are widely used to detect trace amounts of viral RNA in many experiments. In theory, it should be straightforward to assay for viral RNAs of a given sense by using a primer of defined polarity in the RT step of the procedure. For example, if the RT step is primed by an oligonucleotide which binds negative sense viral RNA, cDNA should be produced for subsequent PCR amplification if and only if viral templates of negative sense are present in the original specimen; if negative sense viral RNA is not present, the reaction should be aborted at the RT step, and theoretically no PCR amplification products will be produced.

In fact, several studies have demonstrated that RT-PCR assays based on specific RNA template recognition by RT primers of defined polarity will not reliably distinguish between viral RNAs of positive or negative sense. For example, in control assays using defined hepatitis C virus (HCV) RNA templates, Lanford et al. (1994) demonstrated that an RT-PCR product could be obtained with the ‘incorrect’ sense RT primer or even in the absence of any primer in the RT step. They hypothesized that artifacts arose through a combination of factors, including false priming of the incorrect strand by the RT primer, self-priming of the viral RNA template at regions of secondary structure, and random priming by contaminating or irrelevant nucleic acids. Similarly, Gunji et al. (1994), also working with HCV, showed that conventional RT-PCR assays were not able to reliably detect viral positive and nega-

tive sense RNAs in samples which contained cellular RNAs. These investigators suggested that fragmented cellular RNAs were able to prime viral templates, giving rise to unreliable results.

Despite the findings above, many published research reports are based on conventional RT-PCR assays, relying on the polarity of primers added to the RT step in putative sense-specific measurements of viral RNAs; rarely are control reactions performed to rigorously show that this method is in fact sense-specific. However, upon critical review of the state of available sense-specific RT-PCR assays, McGuinness et al. (1994) indicated ‘... our results clearly establish that reliable detection of HCV-negative RNA strand is not yet achievable by current methods’. Recently, Lerat et al., (1996) demonstrated that even optimized protocols artifactually detect negative sense HCV RNA when these assays are applied to clinical samples. They indicated that artifacts are most likely due to self-priming by abundant viral RNAs in infected tissues. Collectively, these careful studies, using HCV as a model virus, indicate that technical impediments to unambiguous strand-specific RT-PCR determinations of viral RNA may still exist.

In the course of studying the persistence of murine coronaviruses in the mouse central nervous system (Houtman and Fleming, 1996) it was found necessary to determine the sense and amount of viral RNA in the brains of experimental animals. To this end, a RT-PCR procedure was developed and validated which can reliably measure positive and negative sense viral RNA present in trace amounts in a complex biological sample. We describe potential pitfalls of sense-specific RT-PCR assays (ssRT-PCR), as well as techniques introduced by other investigators (Chaves et al., 1994; Lanford et al., 1994; Lerat et al., 1996) and our laboratory to circumvent these artifacts. Finally, the addition of competitor RNA templates to the assay allowed the ssRT-PCR to be performed quantitatively (qssRT-PCR). The method described may easily be adapted to other viral systems, where it is essential to determine the sense and amount of viral RNAs in heterogeneous samples which may contain inhibitory or confounding molecules.

2. Materials and methods

2.1. Virus, cells, animals

All experiments were carried out with murine coronavirus MHV-4, strain 2.2-V-1; (Wang et al., 1992), which was propagated and assayed on DBT cells, as previously described (Fleming et al., 1986). All mice were 6-week-old male C57BL/6J mice (Jackson Laboratory), seronegative for MHV, which were inoculated with 10^3 plaque-forming units (PFUs) of virus intracerebrally. Total cellular RNA was extracted from mouse brains, DBT cells, or FL5 cells which are HeLa cells expressing the MHV receptor (generously provided by Dr Thomas Gallagher, Loyola University, Chicago), using RNA STAT-60 (Tel-test) and following the directions of the manufacturer. Subsequently, RNA was resuspended in DEPC-treated 2 mM EDTA pH 8.0 and stored at -70°C .

2.2. Construction of plasmids containing sequences corresponding to MHV-4 gene 7

Plasmids were constructed for use in *in vitro* RNA transcription to produce control templates for RT-PCR assays. Gene 7 of MHV-4, which codes for the nucleocapsid, or N, protein was chosen as a region of interest. Because of the redundant, 3'-nested structure of coronavirus RNAs (Lai and Cavanagh, 1997), the sequences of gene 7, the most 3' gene, are found in all MHV-4 RNA species. Thus, assaying for RNAs with the targeted N gene sequence will reflect total MHV-4 RNA abundance.

MHV-4 RNA templates were used in RT-PCR reactions to generate two plasmids designated N-wt, corresponding to nucleotides 672–1238 of the MHV-4 N gene, and N-del, containing a 59 bp deletion and an inserted *Bgl* II restriction site relative to N-wt. After RT-PCR amplification, RNA species transcribed from these plasmids or RT-PCR cDNA products made from these template RNAs could be distinguished by size or restriction digestions. However, as the N-wt and N-del derived RNA templates only differed by approximately 10% of their lengths and contained

identical primer binding sites, the amplification efficiencies of the two templates were expected to be nearly equivalent.

Plasmid N-wt was constructed by performing PCR reactions using the Titan RT-PCR system (Boehringer). One microgram of RNA from MHV-4 infected DBT cells was used as the template in RT-PCR reactions primed by 0.2 μM of oligonucleotide primers AM8-1 and AM8-2 (Table 1). In order to facilitate directional ligation, these primers contain short non-viral sequences encoding a 5' *Hind* III or *Kpn* I restriction site respectively. RT was performed at 50°C for 30 min, followed by treatment at 94°C for 2 min. The reactants were then subjected to PCR as per the instructions of the Titan system protocol, and 30 cycles of amplification, each of which consisted of incubation at 94°C for 1 min, 60°C for 1 min, and 72°C for 1 min were performed. After the last PCR cycle, the reaction was held at 72°C for 7 min. PCR products were ethanol precipitated, digested with *Hind* III and *Kpn* I, gel-purified, and ligated into plasmid pGEM-3Z (Promega), which was used to transform competent *Escherichia coli* DH5 α cells. Plasmid N-wt DNA was prepared with the Wizard Maxiprep system (Promega), following the instructions of the manufacturer.

Plasmid N-del was prepared by a similar procedure, except that overlap extension techniques (Ho et al., 1989; Horton et al., 1989; Silver et al., 1995) were used to create the 59 bp deletion and *Bgl* II site relative to N-wt. Briefly, individual PCRs were performed containing 0.2 μM of either primer set (1) AM8-1 and AM8-B or, in the second reaction, (2) AM8-2 and AM8-C (Table 1). The products from reactions (1) and (2) were gel purified, mixed, and subjected to a second PCR utilizing 0.2 μM each of primers AM8-1 and AM8-2. This product was purified subsequently, ligated into pGEM-3Z, and used to produce N-del DNA templates as described above.

2.3. *In vitro* transcription of RNA Templates for RT-PCR

Because pGEM-3Z plasmid (Promega) contains promoters for SP6 and T7 RNA polymerases on opposite sides of the sequences inserted into this

DNA, the system allows in vitro transcription of RNAs from either strand of the DNA, thus producing RNA transcripts which correspond to either sense of the inserted sequences. To produce RNA which corresponded to the positive sense of MHV-4, either N-wt or N-del plasmids were digested with *Eco* RI, and 2.5 µg of the linearized templates were used in an in vitro transcription driven by the RiboMax system (Promega), following the instructions of the manufacturer and utilizing 5 µl of SP6 enzyme mix per 50 µl reaction. Templates corresponding to negative sense of MHV-4 were produced using the same protocol, except that plasmids N-wt or N-del were linearized with *Hind* III, and T7 RNA polymerase was used in the in vitro transcription reactions. After 2 h of incubation, RNA templates were obtained from each reaction by three extractions with phenol:chloroform:isoamyl alcohol (125:24:1, pH 4.7). Subsequently, RNA was precipitated by adjusting NH₄OAc to 2 M, fol-

lowed by the addition of 2.5 volumes of 100% ethanol. After a wash in 75% ethanol, the RNA pellet was resuspended in 25 µl DEPC-treated water. In order to inactivate any residual plasmid template, the RNA suspension was then subjected to a reaction in a 50 µl volume containing 50 mM Tris pH 7.5, 1 mM MnCl₂, 0.5 mg/ml bovine serum albumin, 5 mM DTT, 10 U RNasin (Promega), and 10 U DNase I (Promega). After a 1-h incubation at 37°C, the reaction was terminated by three extractions with phenol:chloroform:isoamyl alcohol (125:24:1, pH 4.7), followed by ethanol precipitation. The RNA pellet was then resuspended in 25 µl 2mM EDTA, pH 8.0, and quantitated by absorbency at 260 nm, as well as by comparison to RNA standards on formaldehyde gels (Promega). RNA was then mixed with two volumes of 100% ethanol, and NaCl was added to achieve a final concentration of 100 mM, after which the sample was stored at –70°C.

Table 1
Sequences and functions of oligonucleotide primers

Name	Purpose ^a	Location ^b	Sequence (5'–3') ^c
AM8-1	Upstream N gene primer	672–693	<i>CCA AGC TTC TGC ACC TGC TAG TCG ATC TG</i>
AM8-2	Downstream N gene primer	1215–1238	<i>CCG GTA CCA CCA TCT TGA TTC TGG TAG GC</i>
AM8-3	Upstream N gene primer for nested RT-PCR	747–768	<i>ATG AAT TCA GCG CCA GCC TGC CTC TAC TG</i>
AM8-4	Downstream N gene primer for nested RT-PCR	1122–1144	<i>ATG GAT CCT GAA TAT TGC AGC TCA TAC AC</i>
AM8-B	Overlap product primer	893–912, 997–1002	<i>TCA GGG AGA TCT GAG TCC TCT TTT GAC GAG GC</i>
AM8-C	Overlap product primer	907–912, 977–996	<i>GGA CTC AGA TCT CCC TGA AAT GTT AAA ACT TG</i>
tag-AM8-1A	RT primer for negative sense N RNA	563–576*, 674–688	<i>GAC GAC AAC AGT GAC TGA ATC TGG, TGC ACC TGC TAG TCG</i>
tag-AM8-2A	RT primer for positive sense N RNA	804–827*, 1216–1230	<i>TCG CAG ACC AAT ACG CAT GAC TCA CCA TCT TGA TTC TGG</i>
IMN-3	upstream tag primer	553–576*	<i>GAC GAC AAC AGT GAC TGA ATC TGG</i>
IMN-4	Downstream tag primer	804–827*	<i>TCG CAG ACC AAT ACG CAT GAC TCA</i>

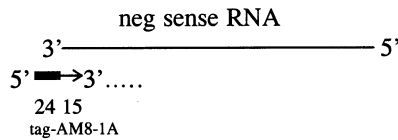
^a Oligonucleotides were used to prime templates corresponding to the N gene of MHV-4 (Genbank database accession number K00757). The irrelevant or tag marker sequences correspond to gene 3 (3a protein and coat protein) of the plant virus cowpea chlorotic mottle virus (CCMV) (Genbank database accession number M28818), control plasmids for which were generously provided by Dr Paul Ahlquist, University of Wisconsin, Madison. Please see text for detailed description of overlap primer use.

^b All sequences correspond to gene N of MHV-4, unless marked with an asterisk, in which case they correspond to gene 3 of CCMV. In most primers, short non-viral sequences were added at the 5' end to create restriction sites and facilitate cloning.

^c Nucleotides which are italicized are non-viral sequences encoding restriction endonuclease recognition sites to facilitate cloning of RT-PCR products. These sequences are, respectively, *Hind* III (AM8-1), *Kpn* I (AM8-2), *Eco*R I (AM8-3), *Bam*H I (AM8-4), and *Bgl* II (AM8-B and AM8-C).

RT Reaction

MMLV, 48°, 60 min

first strand cDNA synthesis,
incorporating 24mer tag**PCR Reaction**

Taq polymerase, 94°/65°/72°, 35 cycles

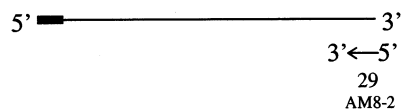
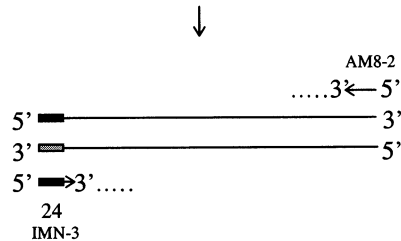
second strand cDNA synthesis,
primed by antiviral 29mer downstream primerselective amplification of templates containing
upstream tag sequences recognized by IMN-3
linked to downstream viral sequences
recognized by AM8-2

Fig. 1. Optimized ssRT-PCR. In this example, the assay for negative sense MHV-4 RNA is shown. Please see text for details and description of assay for positive sense viral RNA. Straight lines represent viral sequences, and boxes represent tag sequences. Numbers under primers or under segments of primers represent their lengths in nucleotides.

2.4. Strand-specific RT-PCR

The following protocol (Fig. 1) was developed after pilot and optimizing experiments. Various amounts of RNA template were mixed with 1 pmol of tag-AM8-2A primer for positive sense amplification or tag-AM8-1A primer for negative sense amplification respectively (Table 1). RT reactions were performed in a final volume of 20 µl containing RNA and primers in a buffer with the following final concentrations: 50 mM Tris-HCl pH 8.3, 75 mM KCl, 3 mM MgCl₂, 10 mM DTT, 0.5 mM dNTPs, 10 U RNasin, and 50 U MMLV reverse transcriptase (Promega). The reaction was incubated at 48°C for 1 h. An AmpliWax PCR gem 100 wax tab (Perkin Elmer) was added to each tube, and the tubes were incubated at 70°C

for 15 min to inactivate the reverse transcriptase. The reactions were then cooled on ice.

An 80 µl mixture was added on top of the wax tab; this solution consisted of 44 mM KCl, 9 mM Tris-HCl pH 9.0, 0.09% Triton X-100, 1.1 mM MgCl₂, 1.25 U *Taq* DNA polymerase (Promega), and 20 pmol primers AM8-1 and IMN-4 for positive sense amplification or primers AM8-2 and IMN-3 (Table 1) for negative sense amplification. The PCR assay was performed in a Perkin Elmer 480 thermal cycler for 35 cycles, each of which consisted of 1 min at 94°C, 1 minute at 65°C, and 1 min at 72°C. At the termination of the PCR, an additional extension reaction was performed at 72°C for 7 min. RT-PCR products were visualized after ethidium bromide staining and electrophoresis on 3% NuSieve (FMC) 3:1

agarose gel or on 1% agarose. Molecular weights of products were estimated by comparison to pUC19 DNA digested separately with *Sau3A I* and *Taq I* restriction endonucleases. For quantitative assays, gels were analyzed by computer-assisted quantitative densitometry (NIH Image, Version 1.61, available at <http://rsb.info.nih.gov/nih-image/>).

2.5. Competitive RT-PCR

Quantification of MHV-4 RNA was achieved by competitive RT-PCR reactions in which a known amount of N-del transcript was added as a standard to each RT reaction. RT-PCR products were visualized by ethidium bromide staining and electrophoresis as described above, and the relative intensity of product bands in each reaction was compared by inspection or by densitometry. Because N-del has a 59 nucleotide deletion relative to genuine MHV-4 sequences, reaction products corresponding to this standard template were easily distinguished from full-length product because their migration in electrophoresis was faster than products derived from N-wt or viral RNA templates. Quantification was achieved either by: (1) comparison of serial dilutions of N-del standard to unknown sample in the equimolar quantitative RT-PCR (qRT-PCR) method to determine the point of equivalence (Gilland et al., 1990); or (2) comparison of an unknown sample's reactivity versus one concentration of N-del in the standard-curve quantitative qRT-PCR method (Tsai and Wiltbank, 1996).

3. Results

3.1. Assay sensitivity and specificity

The optimized protocol above was first used to determine the sensitivity, or limits of detection, for the ssRT-PCR assay. Serial dilutions of *in vitro*-transcribed RNA N-del templates of either positive or negative sense were amplified with specific primers. The optimized ssRT-PCR could detect approximately 1.0 fg of positive sense or negative sense N-del template, either in the pres-

ence (Fig. 2) or absence (data not shown) of 1 μ g of total cellular RNA derived from uninfected DBT cells. Also, we found that the assay for positive sense or negative sense coronavirus RNA did not yield a product when 10⁵ fg of the opposite or 'wrong' sense was added to the reaction (Fig. 2). However, when 10⁶ fg of the inappropriate RNA template was added to the reaction, a non-specific product was detected (data not shown), indicating that the assay has a maximal differential amplification capacity of approximately 100 000-fold with regard to detection of a specific RNA template relative to an excess of inappropriate or opposite sense RNA template. Fig. 3, when compared to Fig. 2, indicates that the inhibition of specific RNA detection in the presence of an excess of wrong sense RNA is insignificant. Finally, in pilot experiments, we have been able to extend the sensitivity of the ssRT-PCR to the attogram (approximately 10 MHV-4 RNA molecules) range by means of nested PCR (Zazzi et al., 1993) methodology using primers AM8-3 and AM8-4 (data not shown); in this case, it is essential in each experiment to include controls of sense specificity, e.g. a control reaction demonstrating the non-amplification of an appropriate concentration of wrong sense RNA.

3.2. Assay precision

The precision, or reproducibility, of the qssRT-PCR assay was determined by testing aliquots of RNA extracted from the brains of an experimental mouse 4 days after MHV-4 inoculation *i.c.* An example of this assay is shown in Fig. 4. The assay for positive sense viral RNA was conducted in the pg range and the negative sense assay conducted in the fg range on the basis of published studies and pilot experiments showing that positive sense coronavirus RNA is in vast excess in most infections. Additional bands were sometimes observed during competitive reactions (Fig. 4); these bands likely represent heteroduplexes (Schneeberger et al., 1995) and were not of sufficient magnitude to interfere with quantification. During densitometric analyses, bands corresponding to heteroduplexes were ignored, as these spe-

cies would be expected to detract from the intensity of both competitor (MHV-4 and N-del) RNAs equally. Three assays were performed by standard curve methodology on separate days (Table 2). As indicated, the coefficients of variation for the positive sense and negative sense assays were 3.0 and 5.7%, respectively. Similar reproducibility was obtained with RNAs obtained from mouse brains during chronic pathogenesis studies and with RNAs derived from infected tissue cultures (data not shown).

3.3. Assay accuracy

Rock (1994) indicates that 'where an accepted standard with a known and agreed upon quantitative result exists, accuracy can be operationally defined as the difference between the measured

value of the standard and the value assigned to the standard'. We initially assessed the accuracy of the qssRT-PCR by carefully determining the concentrations of RNA template stocks by UV absorbency and comparison to commercial RNA standards. Reference standards of positive and negative sense N-wt with an assigned value of 10.0 fg were then prepared and tested in the qssRT-PCR using equimolar methodology in competitions against N-del. The measured values for N-wt standards were 10.2 and 16.5 fg for positive and negative sense templates respectively (versus 10.0 fg, the expected result in a perfect assay, assuming perfect quantification of input RNA stocks against commercial RNA standards).

Unfortunately, it is difficult to produce purified coronavirus genomes in sufficient quantities to serve as biophysically-quantified standards for di-

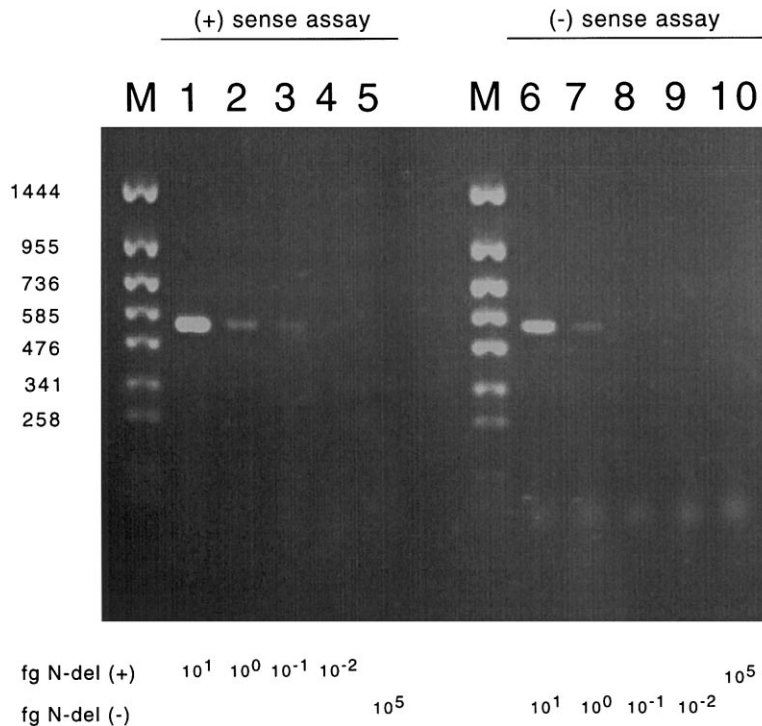


Fig. 2. Sensitivity of ssRT-PCR for positive or negative sense MHV-4 RNA. M, molecular weight markers as described in Section 2. Lanes 1–5, assay for positive sense utilizing 10 fg positive sense (lane 1), 1.0 fg positive sense (lane 2), 0.1 fg positive sense (lane 3), 0.01 fg positive sense (lane 4), and 100 pg negative sense of N-del RNA (lane 5). Lanes 6–10, assay for negative sense utilizing 10 fg of negative sense (lane 6), 1.0 fg of negative sense (lane 7), 0.1 fg of negative sense (lane 8), 0.01 fg of negative sense (lane 9), and 100 pg of positive sense N-del RNA (lane 10). All reactions were performed in the presence of 1 μ g of RNA from uninfected DBT cells.

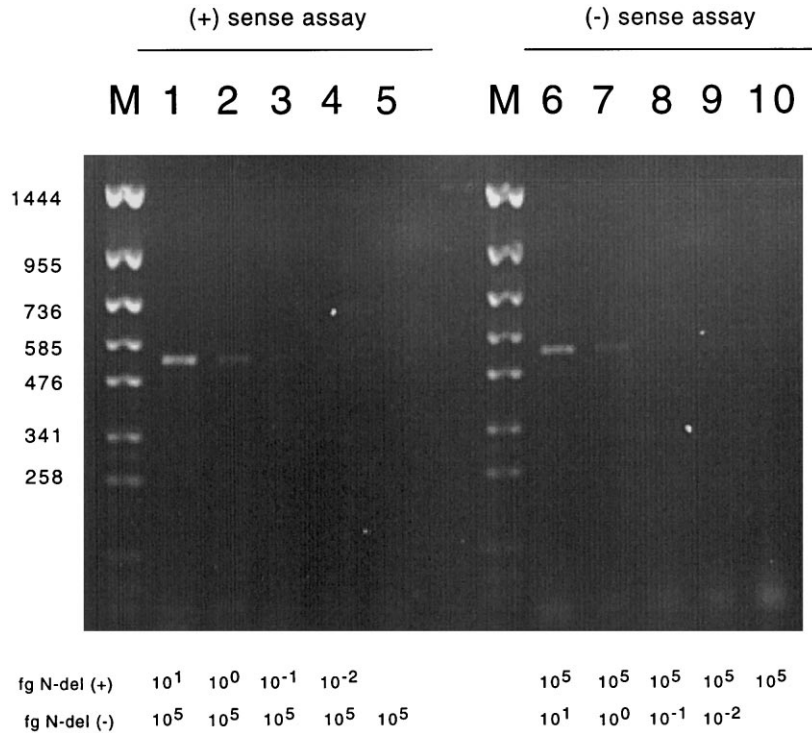


Fig. 3. Minimal inhibition of ssRT-PCR by viral RNAs of opposite sense. M, molecular weight markers. Lanes 1–5, assay for positive sense N-del, performed in the presence of 100 pg negative sense N-del, utilizing 10 fg positive sense (lane 1), 1 fg positive sense (lane 2), 0.1 fg positive sense (lane 3), 0.01 fg positive sense (lane 4) and lane 5, no positive sense N-del RNA. Lanes 6–10, assay for negative sense N-del, performed in the presence of 100 pg positive sense N-del, utilizing 10 fg of negative sense (lane 6), 1.0 fg negative sense (lane 7), 0.1 fg negative sense (lane 8), 0.01 fg of negative sense (lane 9), and no negative sense N-del RNA (lane 10).

rectly assessing the accuracy of our qssRT-PCR versus authentic viral RNA. However, it was possible to isolate and measure viral RNA from FL5 cells after *in vitro* infection by MHV-4 and to compare this result with published results based on established methods. Using equimolar methodology, qssRT-PCR showed that at maximal infection 12 h after inoculation, FL5 cells contained 0.86 ng or 2.7×10^9 molecules of RNA competing with N-del template per microgram of total cellular RNA and, further, that $>99\%$ of the MHV-4 RNA was of positive sense (data not shown). Assuming that the yield of total RNA extracted from FL5 cells was approximately 5.0×10^{-6} μ g of RNA/cell (RNA STAT 60 instructions), on a molar basis these results are in close agreement with prior studies based on hybridization kinetics (Cheley et al., 1981) and Northern blots (Hof-

mann et al., 1990) which indicate that at the peak of coronavirus infection *in vitro* in the order of 10^4 molecules of viral RNA are present in each infected cell. The consistency among different methods of estimating the level of coronavirus expression suggests that the qssRT-PCR assay yields reasonably accurate results when applied to complex biological samples, such as RNA derived from virally-infected cells.

4. Discussion

In studies of coronavirus pathogenesis during chronic viral infection of the murine central nervous system, it was found essential to determine the sense and amount of viral RNA persisting in experimental mice. While RT-PCR in theory

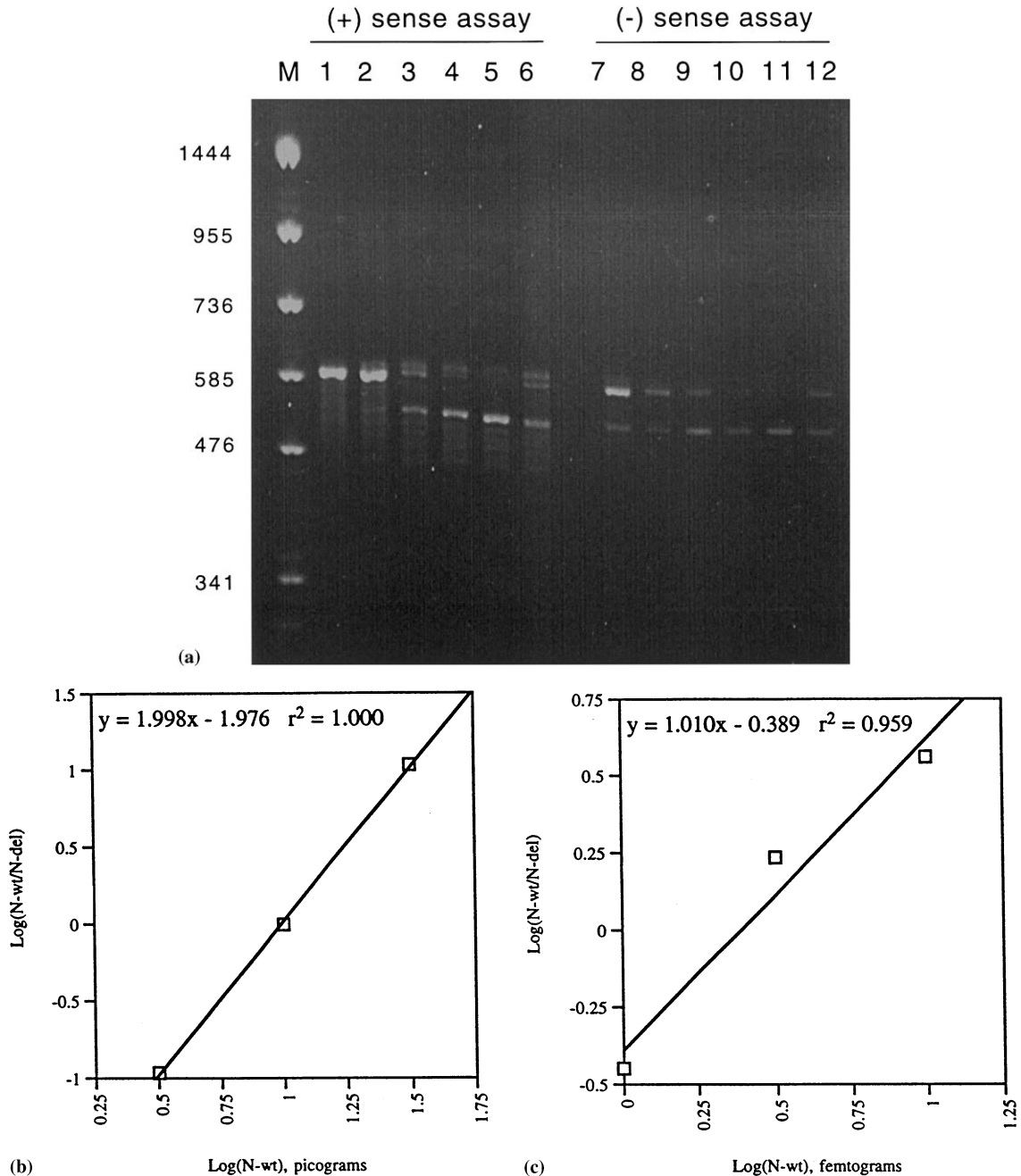


Fig. 4. (a) Determination of MHV-4 RNA in mouse brain 4 days after intracerebral inoculation of virus. Positive (lanes 1–6) or negative (lanes 7–12) sense MHV-4 RNA were assayed by qssRT-PCR, using standard curve methodology, in which a constant amount of competitor RNA (N-del) was amplified with varying amounts of native RNA (N-wt RNA or RNA from infected mouse brain). M, molecular weight markers. In lanes 1–6, 10 pg of positive sense N-del was amplified in the presence of 100 pg positive sense N-wt (lane 1), 31.6 positive sense N-wt (lane 2), 10 pg positive sense N-wt (lane 3), 3.16 pg positive sense N-wt (lane 4), 1 pg positive sense N-wt (lane 5), or 1 μ g brain RNA from a mouse 4 days PI (lane 6). In lanes 7–12, 1 fg of negative sense N-del was amplified in the presence of 10 fg negative sense N-wt (lane 7), 3.16 fg negative sense N-wt (lane 8), 1.0 fg negative sense N-wt (lane 9), 0.316 fg negative sense N-wt (lane 10), 0.1 fg negative sense N-wt (lane 11), or 1 μ g of total brain RNA from the same mouse used for the determination in lane 6 (lane 12). (b) Standard curve of positive sense assay. (c) Standard curve of negative sense assay.

should provide the requisite specificity and sensitivity for these determinations, our initial, exploratory experiments showed that conventional RT-PCR assays for viral RNAs were not sense-specific, let alone quantitative, findings which were concordant with those of previous investigators (Willems et al., 1993). In this regard, most RT-PCR protocols are primarily designed to optimize sensitivity rather than discrimination with regard to RNA template amplification. In other words, in most applications, low levels of amplification of non-specific products are acceptable and do not detract from the primary purpose of the assay, which is efficient detection of the RNA of interest. By contrast, in ssRT-PCR specificity is the over-riding consideration, since the aim of the assay is unambiguous detection of an RNA of a given sense, often under circumstances in which the RNA is orders of magnitude less abundant than an RNA species of the opposite sense (e.g. Table 2). In this case, assay parameters must be such that non-amplification of incorrect sense RNA templates is virtually absolute, since any amplification of the incorrect sense RNA, however infrequent, will be geometrically expanded during PCR and may easily lend to invalid results.

In order to improve the specificity of ssRT-PCR determinations of viral RNA we have adopted and modified several of the procedures described by previous investigators. In our experience, the use of tagged oligonucleotide primers (Chaves et al., 1994; Lanford et al., 1994) was more practical and effective than other proposed specificity-enhancing measures, such as chemical modification of RNA templates (Gunji et al., 1994) or the use of thermostable enzymes, such as *rTth* DNA polymerase, in both RT and PCR

steps (Lanford et al., 1994). The key features of our optimized assay are listed in Table 3. We have found that careful attention to each of these parameters is *imperative* in order to maintain sense-specificity and consistent quantification in the ssRT-PCR. Essentially, during ssRT-PCR there are numerous opportunities for artifacts, and if reliable results are to be obtained, stringent precautions must be taken at every step of the procedure to avoid these artifacts. Furthermore, control samples should be run with every assay in order to be certain that non-specific amplification has not occurred. Crucial methodological parameters of ssRT-PCR are indicated below.

First, a critical consideration in the ssRT-PCR assay developed is the design of oligonucleotide primers for the RT step. These oligonucleotides are hybrid primers in the sense that they contain sequences which are complementary to viral sequences, as well as sequences which are complementary to a non-viral 'tag', or irrelevant, sequence which will be recognized by tag-only primers in the PCR phase of the assay (Fig. 1). Previously reported RT hybrid primers had approximately equal lengths of anti-viral and tag sequences; as a result, RT reactions were performed at 42°C, and PCR annealing temperatures were 46–55°C (Chaves et al., 1994; Lanford et al., 1994; Lerat et al., 1996).

By contrast, we have found it essential to use unbalanced or asymmetrical RT hybrid primers which have short (15–17 mers) anti-viral sequences relative to anti-tag sequences (24–26 mers) (e.g. primer tag-AM8-1A). Pilot experiments demonstrated that symmetrical primers with low PCR annealing temperatures gave rise to non-specific products (data not shown). However,

Table 2
Precision of qssRT-PCR assay^a

	Exp 1	Exp 2	Exp 3	Mean ± S.D.	CV
Positive sense	6.76 pg	7.07 pg	7.28 pg	7.04 ± 0.21 pg	3.0%
Negative sense	1.82 fg	1.82 fg	1.59 fg	1.74 ± 0.10 fg	5.7%

^a Results are expressed in pg of positive sense or fg of negative sense MHV-4 RNA corresponding to the N-wt amplicon/μg of total brain RNA obtained from a mouse 4 days after viral inoculation intracerebrally. Three experiments done by standard curve methodology on separate days are shown, and the results are expressed as the mean and standard deviation (S.D.) for the three assays, as well coefficient of variation (CV) for positive and negative qssRT-PCR assays.

Table 3
Key features of the optimized quantitative sense-specific RT-PCR which affect assay performance

Variable	Optimized parameter	Comments
Design of oligonucleotide primers for RT step	Asymmetrical anti-viral (15–17 mer) and tag (24–26 mer) sequences	Asymmetrical primers allow RT to be performed at 48°C and PCR at 65°C, ensuring high stringency at each step
Relative amount of RT primers compared to PCR primers	1 pmol primer in RT reaction, 20 pmol primers in PCR reaction	Carry-over RT primers are at a relative disadvantage during PCR; in the PCR step, tag primer is in marked excess, assuring specific amplification of correct templates with tag sequences
Reverse transcription, temperature and enzyme	MMLV reverse transcriptase at 48°C for 1 h	MMLV at 42°C has diminished effectiveness with genuine, viral RNA templates; AMV frequently gives rise to non-specific products during RNA sense determination
DNase I treatment of RNA standard templates	Carry-over, confounding plasmid DNA from in vitro transcription reaction is greatly reduced by DNase I digestion in the presence of buffer containing manganese	DNase I only causes single strand nicks of DNA in the presence of Mg ions; with Mn-containing buffer, this enzyme cleaves both strands of DNA
RNA template storage	Minimize freeze–thaw cycles: store in solution at –70°C	Degraded RNA standards or samples will give inaccurate results on qssRT-PCR
Hot start PCR	Reaction tubes always at ≥65°C	Maintaining high temperatures will avoid non-specific binding of PCR primers under conditions of low stringency

in the optimized assay, the RT step is performed at 48°C, close to the melting temperature (TM) of anti-viral sequences of our RT primers, and the PCR annealing step, which depends on longer tag:anti-tag sequence interactions, is set at 65°C. Thus, both the RT and PCR phases of our assay are each conducted under conditions of high stringency, at the threshold at which specific primers are able to anneal correctly to specific templates; in this case, the high stringency in both phases of the assay strongly inhibits non-specific priming.

Another advantage of asymmetrical primers relates to carryover of hybrid RT primers into the PCR phase of the assay. In reported assays in which the anti-viral and tag sequences of the hybrid primers are both approximately 16–18 nucleotides, resulting in RT reaction and PCR annealing temperatures which are close to each other, hybrid RT primers are available and can anneal during the PCR phase of the assay. This availability may result in multiple rounds of cumulative non-specific priming during the PCR, for example, of hybrid primers to aberrant viral RNAs, prior mis-primed products, or to plasmid-derived DNA (in the case of in vitro transcribed RNA standards). In the optimized PCR described, primers carried over from the RT step into the PCR steps are unlikely to misprime, since PCR annealing occurs at temperatures which exceed the TM of viral:anti-viral template:primer interactions but are optimal for specific binding of longer tag:anti-tag sequences. Also, during the PCR phase of the assay, the primers for this step are at 20-fold molar excess relative to primers carried over from the RT step. This discrepancy puts primers from the RT step at a further relative disadvantage during the PCR steps and favors specific tag:anti-tag interactions during the PCR.

Second, we have found that MMLV and 48°C are the optimum combination of reverse transcriptase and temperature for the RT step of our assay. In competitive assays undertaken at lower temperatures, RT of viral RNA was diminished relative to in vitro MHV-4 transcribed templates (e.g. N-del), suggesting that RNA derived from virus may have extensive secondary structure or other features at 42°C which decrease the proces-

sivity of MMLV on this template. Under a variety of conditions, the reverse transcriptase AMV consistently gave rise to non-specific products, thus limiting its applicability in the sense-specific assay described above.

A third methodological consideration relates to the requirement that the specificity of ssRT-PCR assays must be tested with control RNA templates of known sense. Typically, such RNA standards are transcribed in vitro from DNA plasmids. Paradoxically, these control RNA template preparations may introduce artifacts which are not present in actual experimental or clinical samples. For example, traces of plasmid DNA, obviously containing strands of both positive and negative sense, virtually always contaminate RNAs which are transcribed in vitro by conventional protocols; in this case, strand specificity cannot be demonstrated since control reagents themselves are contaminated by sequences of the 'wrong' sense. In order to overcome this problem, it is essential after in vitro transcription of RNA standards to digest the plasmid template with high concentrations of RNase-free DNase in a buffer containing Mn (Bauer et al., 1997) (Table 3). Conventional DNase treatments in Mg-containing buffers did not completely degrade plasmid DNA (data not shown). In our experience, when non-specific products are observed during ssRT-PCR, trouble shooting usually reveals that this artifact is caused by trace contamination of control RNA reagents by residual plasmid DNA. This problem may be corrected by either producing new batches of RNA standards or by repeated DNase treatment of existing RNA standards. Also, the conditions of our RT-PCR assay minimize the possibility of amplification of residual, contaminating plasmid DNA in two other ways. First, during the RT step at 48°C plasmid DNA templates are likely to remain double-stranded and thus are unavailable for amplification. Second, during the PCR step, only primers recognizing tag sequences introduced into prior products will prime *Taq* polymerase (Fig. 1); therefore, carryover plasmid DNA, having exclusively viral sequences and lacking tag sequences, will not be amplified.

Clearly, for assay consistency over time it is necessary to maintain a ribonuclease-free labora-

tory environment (Blumberg, 1987; Jagus, 1987) and to avoid RNA degradation, for example, during tissue extraction, RNA storage, or repeated freeze–thaw cycles of samples (Busch et al., 1992; Farkas et al., 1996; Gill et al., 1996; Halfon et al., 1996). RNA should be isolated immediately, or tissues should be snap-frozen at -70°C . The stability of purified RNA can be maximized by storing stocks as one-use aliquots or as ethanol precipitants at -70°C in dilute NaCl and EDTA. Recent evidence suggests that optimum RNA storage may be achieved in a solution of 1 mM sodium citrate, pH 6.4 (Prediger, 1998). Another essential assay parameter is the institution of a hot start for the PCR, either by means of a heating block (Mullis, 1991) or a wax tab (Perkin Elmer; Chou, et al., 1992), in order to avoid non-specific products which result from priming at low temperatures.

Initially there was considerable, justified scepticism as to the reliability of PCR and related assays with regard to quantitative determination of nucleic acid abundances. However, improved methodology and rigorous control of reactions have permitted unambiguous quantitative PCR and RT-PCR determinations with good correspondence to values obtained with established standard methods, such as Northern blot (Wang et al., 1989; Yokoi, et al., 1993). In fact, the reliability of RT-PCR and similar techniques is such that quantitative assays have been approved for routine clinical use, for example, in determining HIV-1 mRNA levels in patients during antiretroviral chemotherapy (Saag, 1997). In this regard, once the ssRT-PCR assay was optimized, it was relatively straightforward to extend the method to quantitative determinations by adding competitor RNA templates to the reactions. Relative to viral sequences, such competitor RNAs have identical primer binding sites but contain a small deletion which allows specific products generated from these templates to be distinguished on sizing gels. The power of competitive RT-PCR assays is derived from the fact that the sample and competitor RNA templates are amplified in the same reaction tube under identical conditions. Assaying both templates in one tube eliminates sources of error which may occur when control

and experimental templates are amplified in separate tubes and subsequently compared to each other.

Competitive qRT-PCR assays may be run in a variety of formats (reviewed in Köhler et al., 1995), including equimolar methodology (Gilland et al., 1990) and standard curve methodology (Tsai and Wiltbank, 1996). In our assays of coronavirus RNA by qssRT-PCR, we have found that both the equimolar format and standard curve format work well and have similar sensitivity, specificity, precision, accuracy, and practicability (data not shown). We have found it easiest to use the qssRT-PCR in the equimolar mode during initial experiments, when the magnitude of expected coronavirus RNA concentration is unknown. By contrast, the standard curve method has been most convenient at later stages of experiments, when the approximate range of coronavirus RNA concentrations may be anticipated and many replicate samples in this range must be analyzed. Since equimolar and standard curve methods utilize the same reagents and procedures, and differ only in the format in which competitions are conducted, it is easy to switch between these two modes of analysis.

In conclusion, after the requirements for production of tagged primers for sense-specificity and competitor RNA templates for quantification have been met, the assay we have described may easily be performed in any virology laboratory with RT-PCR capabilities. The sense and quantity of any viral RNA may be reliably determined if strict attention is given to controls and to the methodological points listed in Table 3. The assay has been demonstrated to have excellent sensitivity, specificity, and precision, with almost no interference by irrelevant or opposite-sense RNAs. It is more difficult to assess the accuracy, defined as freedom from systematic analytical error or correspondence to a true value (Rock, 1994), of the qssRT-PCR assay we have presented, especially when purified, exactly-quantified standards of genuine viral RNA are not available. The experiments presented demonstrate reasonably accurate assay performance with a variety of conditions and standards, including competitions against RNA obtained during viral infection in

vitro. We suspect that the degree of inaccuracy observed, particularly in the case of negative sense N-wt determinations, is due principally to small errors in measuring the concentrations of our initial RNA template stock solutions. In many applications it may be sufficient to determine if a given viral RNA species is increasing or decreasing relative to a baseline or standard value during the course of an experiment. If, on the other hand, it is essential to know the concentration of a viral RNA in absolute terms, for example, to rigorously determine the average number of viral genomes per infected cell, then additional efforts must be made to precisely measure the concentration of competitor RNA standards, followed by careful titration of these standards in competitions against actual viral RNAs under realistic experimental conditions.

Acknowledgements

We would like to thank Dr Thomas Gallagher for the gift of FL5 cells and Dr Mary Lokuta for helpful discussions and suggestions. We also thank Meera Nathan and Joan Pooley for excellent technical assistance, and Nola Mills for excellent editorial assistance. This work was funded by a Merit Review Grant from the Veterans Administration and by Research Grant RG 2283-B-3 from the National Multiple Sclerosis Society.

References

- Ausubel, F.M., Brent, R., Kingston, R.E., Moore, D.D., Seidman, J.G., Smith, J.A., Struhl, K. (Eds.), 1994. *Current Protocols in Molecular Biology*, Wiley, New York, pp. 4.9.12.
- Bauer, P., Rolfs, A., Regitz-Zagrosek, V., Hildebrandt, A., Fleck, E., 1997. Use of manganese in RT-PCR eliminates PCR artifacts resulting from DNase I digestion. *BioTechniques* 22, 1128–1132.
- Blumberg, D.D., 1987. Creating a ribonuclease-free environment. *Methods Enzymol.* 152, 20–24.
- Busch, M.P., Wilber, J.C., Johnson, P., Tobler, L., Evans, C.S., 1992. Impact of specimen handling and storage on detection of hepatitis C virus RNA. *Transfusion* 32, 420–425.
- Chaves, R.L., Graff, J., Normann, A., Flehmig, B., 1994. Specific detection of minus strand hepatitis A virus RNA by Tail-PCR following reverse transcription. *Nucleic Acids Res.* 22, 1919–1920.
- Cheley, S., Anderson, R., Cupples, M.J., Lee Chan, E.C.M., Morris, V.L., 1981. Intracellular murine hepatitis virus-specific RNAs contain common sequences. *Virology* 112, 596–604.
- Chou, Q., Russell, M., Birch, D., Raymond, J., Bloch, W., 1992. Prevention of pre-PCR mis-priming and primer dimerization improves low-copy-number amplifications. *Nucleic Acids Res.* 20, 1717–1723.
- Farkas, D.H., Kaul, K.L., Wiedbrauk, D.C., Kiechle, F.L., 1996. Specimen collection and storage for diagnostic molecular pathology investigation. *Arch. Pathol. Lab. Med.* 120, 591–596.
- Fleming, J.O., Trousdale, M.D., El-Zaatari, F.A.K., Stohlman, S.A., Weiner, L.P., 1986. Pathogenicity of antigenic variants of murine coronavirus JHM selected with monoclonal antibodies. *J. Virol.* 58, 869–875.
- Foley, K.P., Leonard, M.W., Engel, J.D., 1993. Quantitation of RNA using the polymerase chain reaction. *Trends Genet.* 9, 380–385.
- Gill, S.S., Aubin, R.A., Bura, C.A., Curran, I.H.A., Matula, T.I., 1996. Ensuring recovery of intact RNA from rat pancreas. *Mol. Biotech.* 6, 359–362.
- Gilland, G., Perrin, S., Bunn, H.F., 1990. Competitive PCR for quantitation of mRNA. In: Innis, M.A., Gelfand, D.H., Sninsky, J.J., White, T.J. (Eds.), *PCR Protocols*. Academic Press, San Diego, pp. 60–69.
- Gunji, T., Kato, N., Hijikata, M., Hayashi, K., Saitoh, S., Shimotohno, K., 1994. Specific detection of positive and negative stranded hepatitis C viral RNA using chemical RNA modification. *Arch. Virol.* 134, 293–302.
- Halfon, P., Khiri, H., Gerolami, V., Bourliere, M., Feryn, J.M., Reynier, P., Gauthier, A., Cartouzou, G., 1996. Impact of various handling and storage conditions on quantitative detection of hepatitis C virus RNA. *J. Hepatol.* 25, 307–311.
- Ho, S.N., Hunt, H.D., Horton, R.M., Pullen, J.K., Pease, L.R., 1989. Site directed mutagenesis by overlap extension using the polymerase chain reaction. *Gene* 77, 51–59.
- Hofmann, M.A., Sethna, P.B., Brian, D.A., 1990. Bovine coronavirus mRNA replication continues throughout persistent infection in cell culture. *J. Virol.* 64, 4108–4114.
- Horton, R.M., Hunt, H.D., Ho, S.N., Pullen, J.K., Pease, L.R., 1989. Engineering hybrid genes without the use of restriction enzymes: gene splicing by overlap extension. *Gene* 77, 61–68.
- Houtman, J.J., Fleming, J.O., 1996. Pathogenesis of mouse hepatitis virus-induced demyelination. *J. NeuroVirol.* 2, 361–376.
- Jagus, R., 1987. Hybrid selection of mRNA and hybrid arrest of translation. *Methods Enzymol.* 152, 567572.
- Köhler, T., Lassner, D., Rost, A.-K., Thamm, B., Pustowoit, B., Remke, H. (Eds.), 1995. *Quantification of mRNA by Polymerase Chain Reaction*, Springer, Berlin.

- Lai, M.M.C., Cavanagh, D., 1997. The molecular biology of coronaviruses. *Adv. Virus Res.* 48, 1–100.
- Lanford, R.E., Sureau, C., Jacob, J.R., White, R., Fuerst, T.R., 1994. Demonstration of in vitro infection of chimpanzee hepatocytes with hepatitis C virus using strand-specific RT-PCR. *Virology* 202, 606–614.
- Lerat, H., Berby, F., Traubaud, M.-A., Vidalin, O., Major, M., Trépo, C., Inchauspé, G., 1996. Specific detection of hepatitis C virus minus strand RNA in hematopoietic cells. *J. Clin. Invest.* 97, 845–851.
- McGuinness, P.H., Bishop, G.A., McCaughan, G.W., Trowbridge, R., Gowans, E.J., 1994. False detection of negative-strand hepatitis C virus RNA. *Lancet* 343, 551–552.
- Mullis, K., 1991. The polymerase chain reaction in an anemic mode: how to avoid cold oligodeoxyribonuclear fusion. *PCR Methods Appl.* 1, 1–4.
- Prediger, E., 1998. RNA isolation: new ways to handle tissue and store RNA. *Ambion TechNotes* 5, 1–16.
- Rock, R.C., 1994. Technical evaluation of laboratory studies. In: Noe, D.A., Rock, R.C. (Eds.), *Laboratory Medicine: The Selection and Interpretation of Clinical Laboratory Studies*. Williams and Wilkins, Baltimore, pp. 15–26.
- Saag, M.S., 1997. Quantification of HIV viral load: a tool for clinical practice. In: Sande, M.A., Volberding, P.A. (Eds.), *The Medical Management of AIDS*. W.B. Saunders, Philadelphia, pp. 57–74.
- Schneeberger, C., Speiser, P., Kury, F., Zeillinger, R., 1995. Quantitative detection of reverse transcriptase-PCR products by means of a novel and sensitive DNA stain. *PCR Methods Appl.* 4, 234–238.
- Silver, J., Limjoco, T., Feinstone, S., 1995. Site-specific mutagenesis using the polymerase chain reaction. In: Innis, M.A., Gelfand, D.H., Sninsky, J.J. (Eds.), *PCR Strategies*. Academic Press, San Diego, pp. 179–188.
- Tsai, S.-J., Wiltbank, M.C., 1996. Quantification of mRNA using competitive RT-PCR with standard curve methodology. *BioTechniques* 21, 862–866.
- Wang, A.M., Doyle, M.V., Mark, D.F., 1989. Quantitation of mRNA by the polymerase chain reaction. *Proc. Natl. Acad. Sci. USA* 86, 9717–9721.
- Wang, F.I., Fleming, J.O., Lai, M.M.C., 1992. Sequence analysis of the spike protein gene of murine coronavirus variants: study of genetic sites affecting neuropathogenicity. *Virology* 186, 742–749.
- Willems, M., Moshage, H., Yap, S.H., 1993. PCR and detection of negative HCV RNA strands. *Hepatology* 17, 526.
- Yokoi, H., Natsuyama, S., Iwai, M., Noda, Y., Mori, T., Mori, K.J., Fujita, K., Nakayama, H., Fujita, J., 1993. Non-radioisotopic quantitative RT-PCR to detect changes in mRNA levels during early mouse embryo development. *Biochem. Biophys. Res. Commun.* 195, 769–775.
- Zazzi, M., Romano, L., Peruzzi, F., Toneatto, S., De Milito, A., Botta, G., Valensin, P.E., 1993. Optimal conditions for detection of human immunodeficiency virus type 1 DNA by polymerase chain reaction with nested primers. *Mol. Cell. Probes* 7, 431–437.